GEOPHYSICS, VOL. 44, NO. 4 (APRIL 1979); P. 681–690, 11 FIGS., 1 TABLE

Attenuation of seismic waves in dry and saturated rocks: I. Laboratory measurements

M. N. Toksöz,* D. H. Johnston*, and A. Timur‡

The attenuation of compressional (P) and shear (S) waves in dry, saturated, and frozen rocks is measured in the laboratory at ultrasonic frequencies. A pulse transmission technique and spectral ratios are used to determine attenuation coefficients and quality factor (Q) values relative to a reference sample with very low attenuation. In the frequency range of about 0.1–1.0 MHz, the attenuation coefficient is linearly proportional to frequency (constant Q) both for P- and S-waves. In dry rocks, Q_p of compressional waves is slightly smaller than Q_s of shear waves. In brine and water-saturated rocks, Q_p is larger than Q_s. Attenuation decreases substantially (Q values increase) with increasing differential pressure for both P- and S-waves.

INTRODUCTION

The attenuation of compressional (P) and shear (S) waves in rocks strongly depends on the physical state and saturation conditions. Generally, attenuation varies much more than the seismic velocities as a result of changes in the physical state of materials. Thus, the anelastic properties of rocks supplement the elastic when inferring saturation conditions and pore fluids by seismic techniques. However, the experimental determination of attenuation is more difficult than the measurement of velocities.

Attenuation measurements have been carried out in the laboratory using different techniques over a fairly wide frequency range (Attewell and Ramana, 1966; Birch and Bancroft, 1938; Born, 1941; Bradley and Fort, 1966; Gardner et al, 1964; Hamilton, 1972; Jackson, 1969; Knopoff, 1964; Nur and Simmons, 1969; Peselnick and Zietz, 1959; Peselnick and Outerbridge, 1961; Spetzler and Anderson, 1968; Tittmann et al, 1974; Tullos and Reid, 1969; Warren et al, 1974; Watson and Wuenschel, 1973; Wyllie et al, 1962). These measurements indicate the attenuation coefficient is generally proportional to frequency (i.e., the quality factor Q is independent of frequency). Data on the dependence of attenuation on fluid saturation and pressure are relatively scarce. Available measurements indicate that (1) fluid saturation increases attenuation (Gardner et al, 1964; Wyllie et al, 1962; Obert et al, 1946; Watson and Wuenschel, 1973), and (2) increasing pressure decreases attenuation (Gardner et al, 1964; Gordon and Davis, 1968; Levykin, 1965; Klima et al, 1964). However, more laboratory data are needed under controlled conditions to determine the effects of fluids and pressure on the attenuation in porous rocks.

In this paper, we present laboratory data on attenuation and its dependence on fluid saturation (methane, water, brine) and pressure. Part II of this paper (Johnston et al, 1979, this issue), discusses the mechanisms of attenuation and formulates theoretical models that fit the laboratory data.

ATTENUATION MEASUREMENTS

Accurate measurement of intrinsic attenuation is a difficult task and seriously limits the utilization of anelastic rock properties. Both in the laboratory and in the field, seismic wave amplitudes are strongly affected by geometric spreading, reflections, and scattering in addition to intrinsic damping. Thus, to obtain the true attenuation, it is necessary to correct for these other effects; this can be a formidable task.

In the laboratory, attenuation is generally measured by one of several techniques. These include the resonant bar method (Birch and Bancroft, 1938; Born, 1941; Gardner et al, 1964; Spetzler and Anderson,

Manuscript received by the Editor July 30, 1977; revised manuscript received February 27, 1978.
*Department of Earth and Planetary Sciences, M.I.T., Cambridge, MA 02139.
‡Chevron Oil Field Research Co., Box 446, La Habra, CA 90631.
0016-8033/79/0401—0681$03.00.

1968); amplitude decay of multiple reflections (Peselnick and Zietz, 1959); slow stress strain cycling (Jackson, 1969); or a pulse transmission method where the amplitude decay of seismic signals traveling through samples is measured (Kuster and Toksöz, 1974; Tittmann et al, 1974; Watson and Wuenschel, 1973).

The pulse transmission technique is most suited for use in pressure vessels with jacketed and saturated samples, provided correction can be made for geometric factors such as beam spreading and reflections. We use the pulse transmission technique and measure attenuation relative to a reference sample which has very low attenuation. A description of the laboratory setup and high-pressure system is given by Timur (1977). The samples used in this Acoustic Measurements System (AMS) are cylindrical and generally 8.9 cm in diameter and 5.1 cm in length. Transmitter and receiver transducers (each 2.5 cm in diameter) are mounted at opposite ends of the samples. Only one-way transmission effects are measured. The sample to be studied and the reference sample have exactly the same shape and geometry. Essentially, two measurements are made using identical procedures, one with the rock sample of interest and the second with the reference sample.

The amplitudes of plane seismic waves for the reference and the sample can be expressed as

$$A_1(f) = G_1(x)e^{-\alpha_1(f)x}\, e^{i(2\pi ft - k_1 x)},$$

and (1)

$$A_2(f) = G_2(x)e^{-\alpha_2(f)x}\, e^{i(2\pi ft - k_2 x)},$$

where A = amplitude, f = frequency, x = distance, $k = 2\pi f/v$ = wavenumber, v = velocity, $G(x)$ is a geometrical factor which includes spreading, reflections, etc., and $\alpha(f)$ is the frequency-dependent attenuation coefficient. Subscripts 1 and 2 refer to the reference and sample, respectively. From available data it is reasonable to assume that over the frequency range of the measurements, 0.1–1.0 MHz, α is a linear function of frequency, although the method itself tests this assumption (Knopoff, 1964; Jackson and Anderson, 1970; McDonal et al, 1958). Thus one can write:

$$\alpha(f) = \gamma f, \tag{2}$$

where γ is constant and related to the quality factor Q by

$$Q = \frac{\pi}{\gamma v}. \tag{3}$$

When the same geometry is used for both the sample and standard (i.e., same sample dimensions, transducers, and arrangements), then G_1 and G_2 are frequency-independent scale factors. The ratio of the Fourier amplitudes is:

$$\frac{A_1}{A_2} = \frac{G_1}{G_2} e^{-(\gamma_1 - \gamma_2)fx}, \tag{4}$$

or

$$\ln\left(\frac{A_1}{A_2}\right) = (\gamma_2 - \gamma_1)xf + \ln\left(\frac{G_1}{G_2}\right), \tag{5}$$

where x is the sample length.

When G_1/G_2 is independent of frequency, $(\gamma_2 - \gamma_1)$ can be found from the slope of the line fitted to $\ln(A_1/A_2)$ versus frequency. If the Q of the standard reference is known, γ_2 of the sample can be determined. When the Q of the standard is very high (i.e., $Q_1 \cong \infty$), then $\gamma_1 = 0$, and γ_2 of the rock sample can be determined directly from the slope.

With the exception of the first set of measurements reported below, aluminum was used as the standard reference. Q for aluminum is about 150,000 (Zam-

Table 1. Measured porosities, velocities, and quality factors of three rock samples.

	Porosity (percent)	Velocities (km/sec) V_p	V_s	Quality factors* Q_p	Q_s
Navajo sandstone	12.5				
Room temperature		4.25	2.38	7.3	6.2
Frozen		5.59	3.63	—	—
Boise sandstone	25.0				
Room temperature		3.42	1.90	6.9	6.1
Frozen		4.92	2.90	—	—
Spergen limestone	14.8				
Room temperature		4.70	2.49	14.9	12.1
Frozen		5.83	3.12	—	—

*Assuming Q in frozen state is very high ($Q_{\text{frozen}} \cong \infty$)

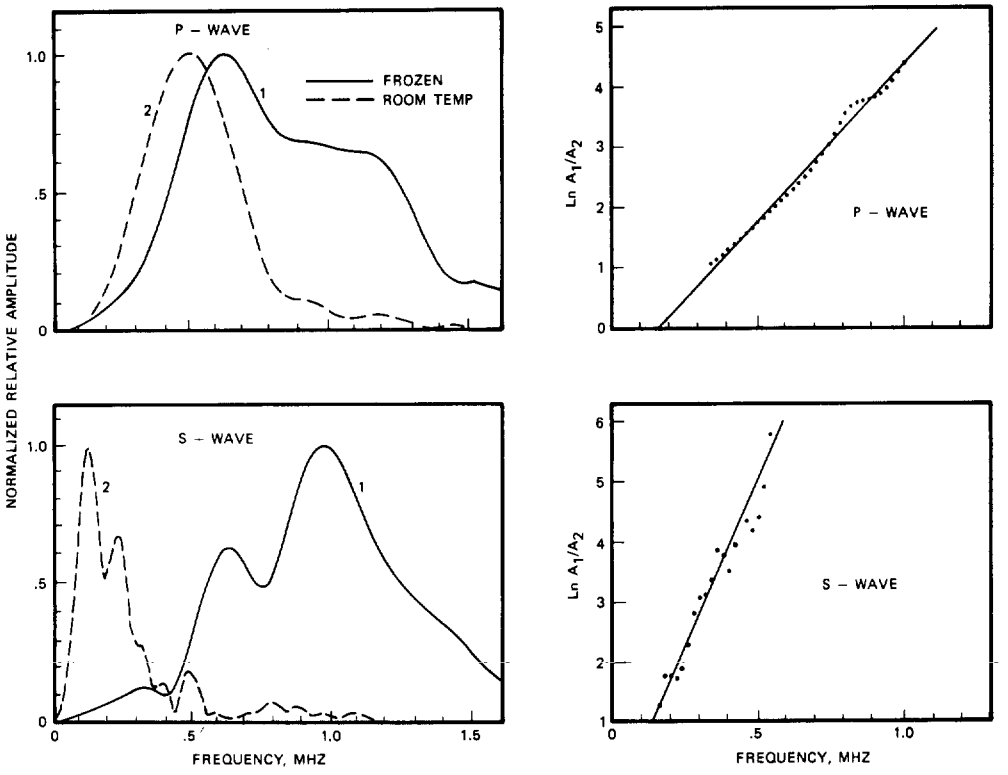

FIG. 1. Attenuation characteristics of the Navajo sandstone. Amplitude spectra and the natural logarithm of the spectral ratios versus frequency for frozen at $T = -40°C$ (curve 1) and water-saturated at room temperature (curve 2) samples. The top figure is compressional waves and the bottom figure shear waves.

anek and Rudnick, 1961), as opposed to $Q \leq 1000$ for rocks. Thus, taking $\gamma_1 = 0$ never introduces more than 1 percent error. For typical rocks where $Q = 10–100$, the error is less than 0.1 percent and is negligible. A more serious concern is the validity of the assumption that the geometric factors G_1 and G_2 have the same frequency dependence, and G_1/G_2 is independent of frequency. With polished rock surfaces and good coupling between the transducer holder and sample, one would not expect frequency-dependent reflection coefficients at the interface. Repeated measurements showed that pulse amplitudes, shapes, and spectra were duplicated. As a further test of the experimental method, Q values for Lucite were obtained using both the spectral ratios and a dynamic resonance technique. The results were in good agreement with $Q_p \approx Q_s \approx 50$. Finally, Q values using spectral ratios were found for Lucite and a Berea sandstone relative to aluminum for 1, 2, and 3 inch sample lengths. The measurements were done with uniaxial pressure. In each case, the Q values for P- and S-waves obtained with different length samples were consistent, supporting the assumption of a frequency independent G_1/G_2.

LABORATORY MEASUREMENTS

Two types of measurements were carried out in this study:

(1) Attenuation of P- and S-waves at one atm pressure in water-saturated and frozen sandstone and limestone samples; and

(2) attenuation of P- and S-waves as a function of pressure in a dry, gas, and brine-saturated Berea sandstone.

The purpose of the first set of measurements was to determine effects of lithology and porosity on attenuation in different rock types. The second set of measurements was important for understanding the mechanisms of attenuation and for extrapolating laboratory data to field applications.

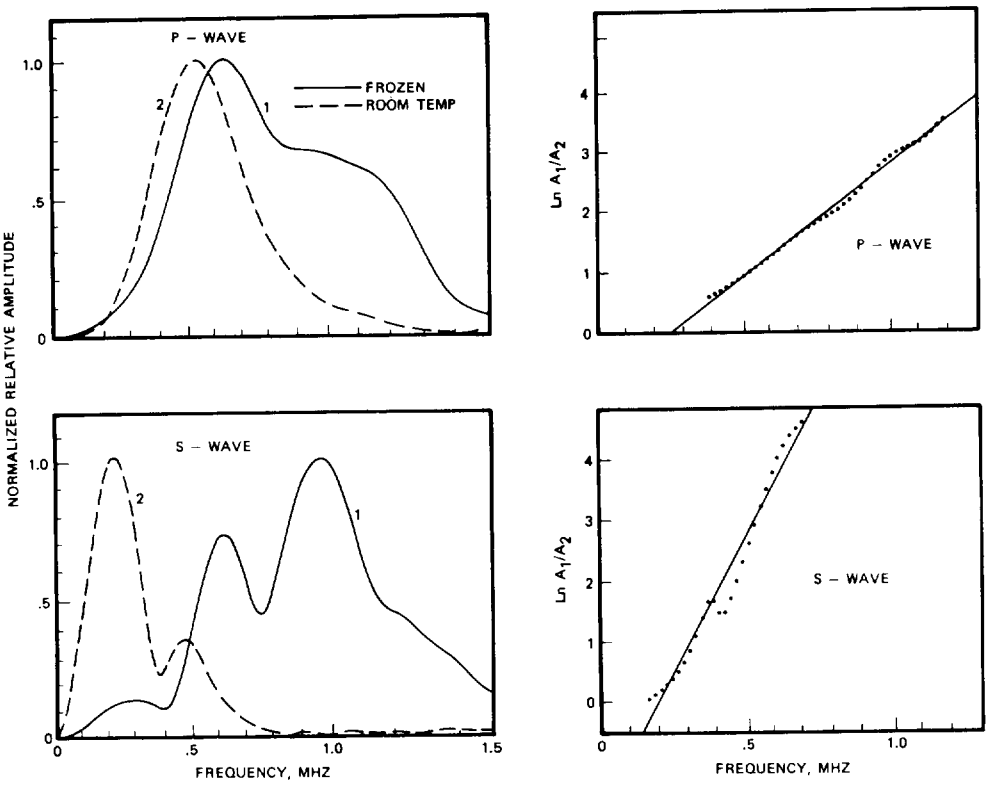

FIG. 2. Attenuation characteristics of the Spergen limestone. Curves are as described in Figure 1.

Attenuation measurements of water-saturated and frozen samples

Seismic velocities and Fourier spectra of *P*- and *S*-waves for three rocks were determined at 1 atm confining pressure saturated with water first at room temperature and then in the frozen state at −40°C. The three rocks, Navajo and Boise sandstones and Spergen limestone, have porosities and measured velocities listed in Table 1. The experimental technique and velocity measurements are discussed in an earlier paper (Toksöz et al, 1976). In this section we emphasize the attenuation data.

The samples were jacketed with a thin rubber sleeve and then saturated with distilled water using a vacuum technique. *P*- and *S*-wave velocities were measured and the waveforms were recorded with the sample at room temperature (+20°C). The samples were then frozen and maintained at −40°C while similar measurements were made. After this, the samples were brought back to room temperature and measurements were repeated. The repeated measurements of velocities at room temperature before and after freezing agreed to within 1 percent for *P*-waves and to within 2 percent for *S*-waves for all rocks, except for the Spergen limestone, for which velocities were lowered by about 5 percent as a result of the freezing cycle, indicating some matrix damage and crack formation as a result of freezing.

From the waveform spectra shown in Figures 1 and 2, it is clear that the attenuation is much greater in the room temperature case. In frozen rocks, attenuation is very small and Q is very high (Spetzler and Anderson, 1968). Thus, we use the frozen rock as a reference standard and determine Q in the water-saturated case relative to the frozen state with the spectral ratio method discussed in the previous section. Q in frozen rocks is greater than 100. For this lower limit, the relative Q values for water-saturated rocks may be about 10 percent higher than the absolute values. If Q in the frozen state is 500, relative Q is within 3 percent of the absolute value.

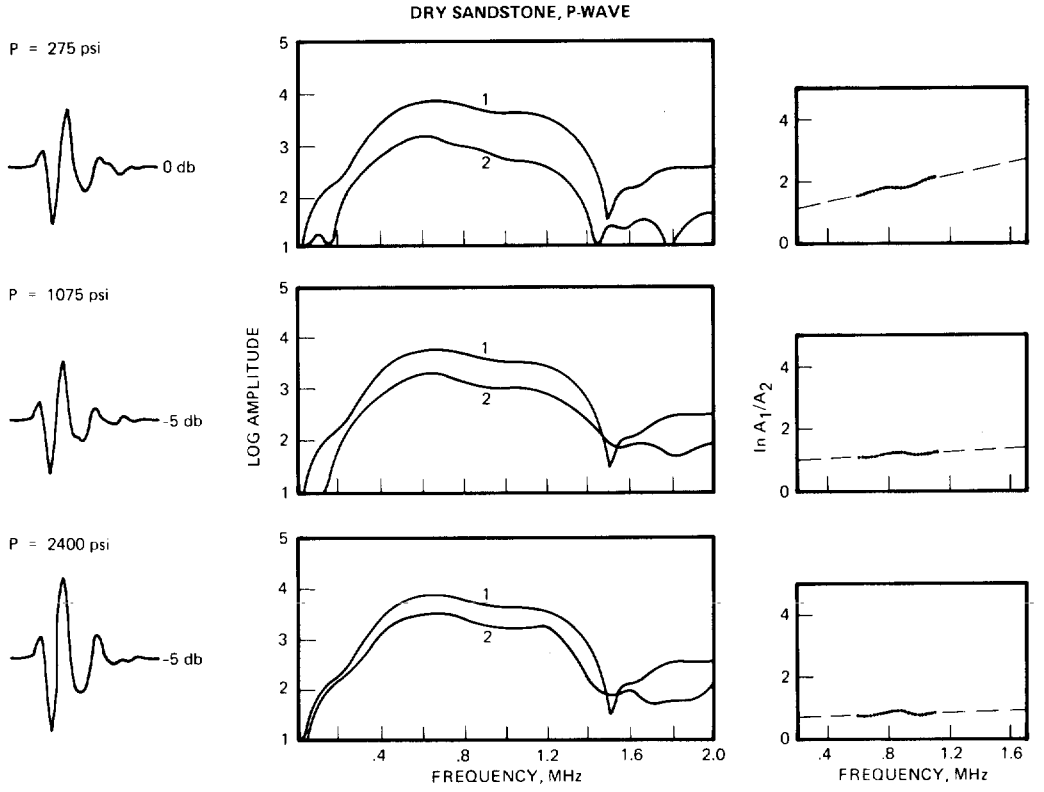

FIG. 3. Attenuation characteristics of P-waves in dry Berea sandstone at three different confining pressures: $P_c = 275$, 1075, 2400 psi ($P_f = 0$, thus $P_d = P_c$). Left: pulse waveforms in sandstone. Center: logarithm of Fourier amplitude as a function of frequency. Curve 1 is the aluminum reference and curve 2 is the rock. Right: natural logarithm of the aluminum to rock amplitude ratios as a function of frequency. The closely spaced points are actual ratios and the dashed line is the linear fit to the data. γ and Q are calculated from the slope of this line.

An examination of the Q values tabulated in Table 1 shows that, in water-saturated (unfrozen) rocks at 1 atm confining pressure for the samples studied; (1) Q of S-waves (Q_s) is slightly lower than Q of P-waves (Q_p) in all three samples; (2) in sandstones, Q decreases with increasing porosity but the decrease is small; and (3) for a given porosity, limestone has a higher Q than sandstone.

Attenuation measurements as a function of pressure and saturation

To determine the effects of pressure and saturating fluids on the attenuation properties of porous rocks, a detailed experiment was conducted with a Berea sandstone. The sample used has a porosity of 16 percent, permeability of 75 mD, and a matrix density of 2.61 g/cm. Berea is a relatively clean sandstone, and a petrographic description of it is given by Timur (1968).

In the following experiments, jacketed samples were placed in a pressure vessel (Timur, 1977) where pore fluid pressure (P_f) and confining pressure (P_c) are controlled independently within a range of 0–3 kb. Measurements were made at discrete differential pressures ($P_d = P_c - P_f$) with sufficient time between measurements for the sample to reach equilibrium. Both increasing and decreasing pressure directions are used to test for repeatibility, hysteresis, or any indication of sample damage.

Attenuation and velocity measurements were made as described before in the differential pressure range of 1 bar to 550 bars (8000 psi) in dry, methane, and brine-saturated samples. An aluminum sample with the same shape as the Berea sandstone sample was

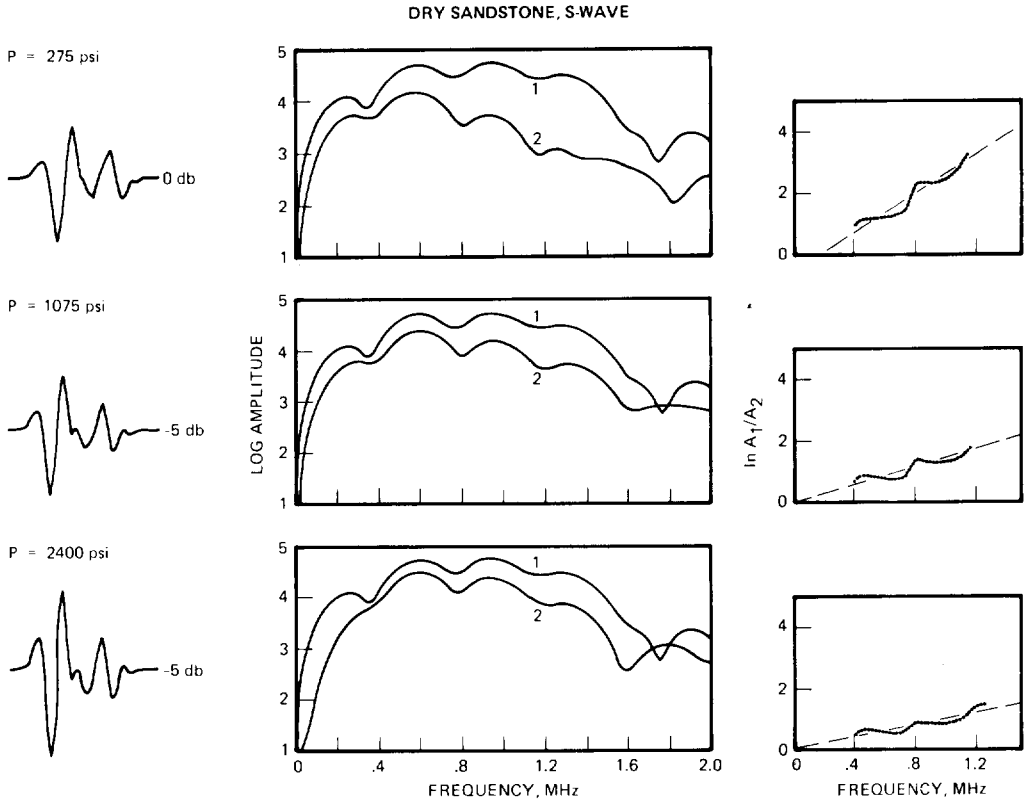

FIG. 4. Attenuation characteristics of S-waves in dry Berea sandstone. See Figure 3 for explanations.

used as a standard reference. Q values were calculated from spectral ratios of rock-aluminum pairs at each pressure.

In the first experiment, the sample was dried in a vacuum oven at 80°C, at a pressure of 50 μm of mercury while being periodically flushed with argon. P- and S-wave traveltimes and full waveforms were recorded in the confining pressure range of 1 bar (14.7 psi) to 550 bars (8000 psi) for both the rock sample and aluminum standard ($P_f = 0$; therefore, $P_d = P_c$). Examples of pulse waveforms, spectra, and spectral ratios at three confining pressures are shown in Figures 3 and 4 for P- and S-waves, respectively. The decrease of the attenuation coefficient (decreasing slope of the spectral ratio) with increasing pressure is obvious from these figures. Measured velocities as a function of pressure are shown in Figure 5 (Jones et al, 1977). Q values were calculated from the slopes of spectral ratios and velocities, and are shown in Figure 6. Both Q_p and Q_s increase rapidly with confining pressure with a slight leveling off at higher pressures. Also, in this dry case, Q_s is slightly higher than Q_p.

In the second experiment, the sample was fully saturated with methane and the experiment repeated with $P_f = 0.465\ P_c$. This ratio of pore-fluid to confining pressures is a nominal value for saturated sedimentary rocks where the pore-fluid pressure is equal to the hydrostatic pressure of a water column. The behavior of the spectra and spectral ratios for methane-saturated rocks was similar to those shown in Figures 3 and 4. The resulting Q values are plotted as a function of differential pressure in Figure 7. Q_p increases rapidly at first with pressure but appears to level off at higher pressures. Q_s is again either equal to or slightly larger than Q_p. It exhibits a similar but slightly more gradual behavior. As would be expected, the differences between the dry rock and the methane-saturated rock are small.

Following the methane run, the sample was com-

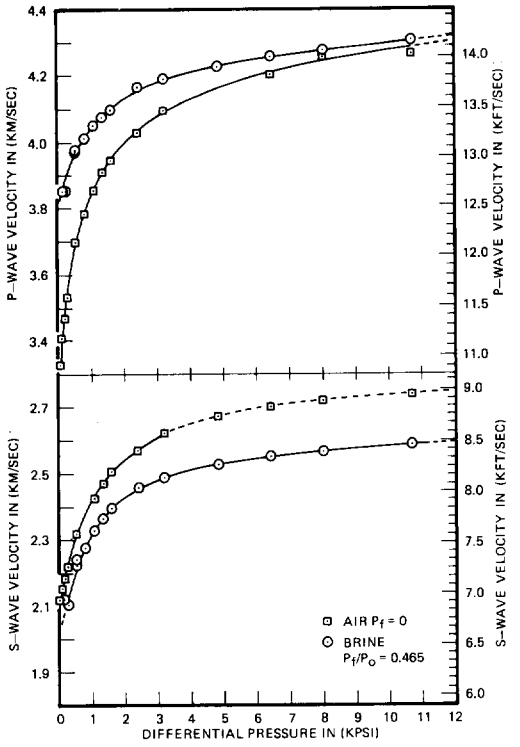

FIG. 5. Velocities of P- and S-waves as a function of differential pressure in dry and brine-saturated Berea sandstone. These velocities are used for the Q calculations.

pletely saturated with an NaCl brine of 67,191 ppm concentration. Again, P_f was maintained at 0.465 P_c throughout the experiment. Pulse waveforms, spectra, and spectral ratios are shown for three values of differential pressure in Figures 8 and 9 for P- and S-waves. An increase of the attenuation coefficient relative to the dry case (Figures 3 and 4) is obvious from the spectral ratios. Q values obtained are shown as a function of differential pressure in Figure 10. The same behavior as seen in Figures 6 and 7 is observed here. In the brine-saturated case, however, Q_s is lower than Q_p. This is in agreement with earlier results listed in Table 1, and it shows that this behavior for saturated rocks holds at high pressures as well.

A final brine-saturated (NaCl = 161,334 ppm) experiment was run in which P_c was fixed at 1035 bars (15,000 psi) and P_f was decreased from 1000 bars (14,500 psi). The results are shown in Figure 11 and are similar to those obtained in the previous experiment (Figure 10) at lower pressures ($P_d \leq$ 8000 psi). However, at a pressure of about $P_d =$ 13,000 psi, there is a definite increase in Q. This is most likely due to collapse of some of the thicker pore spaces and complete locking of some grain boundaries.

The interpretation of these results in terms of attenuation mechanisms is discussed in Part II. These data, in fact, provide strong constraints for determining the relative contributions of different mechanisms for attenuation of seismic waves in rock under different saturation conditions.

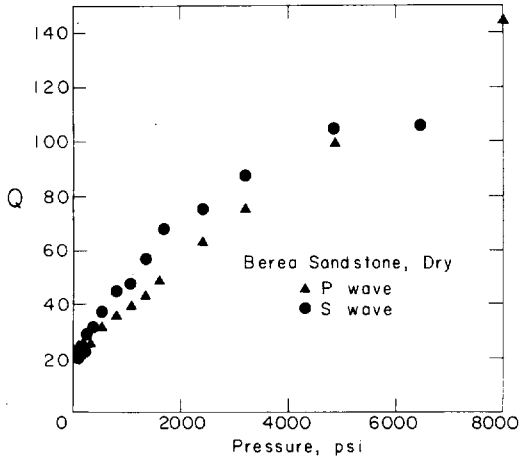

FIG. 6. Q values of P- and S-waves as a function of confining pressure in dry Berea sandstone ($P_f = 0$).

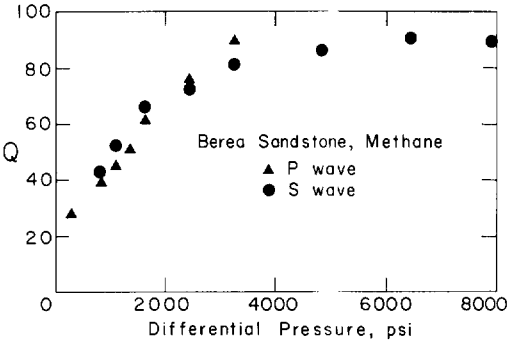

FIG. 7. Q-values of P- and S-waves as a function of differential pressure in methane saturated Berea sandstone ($P_f = 0.465\ P_c$).

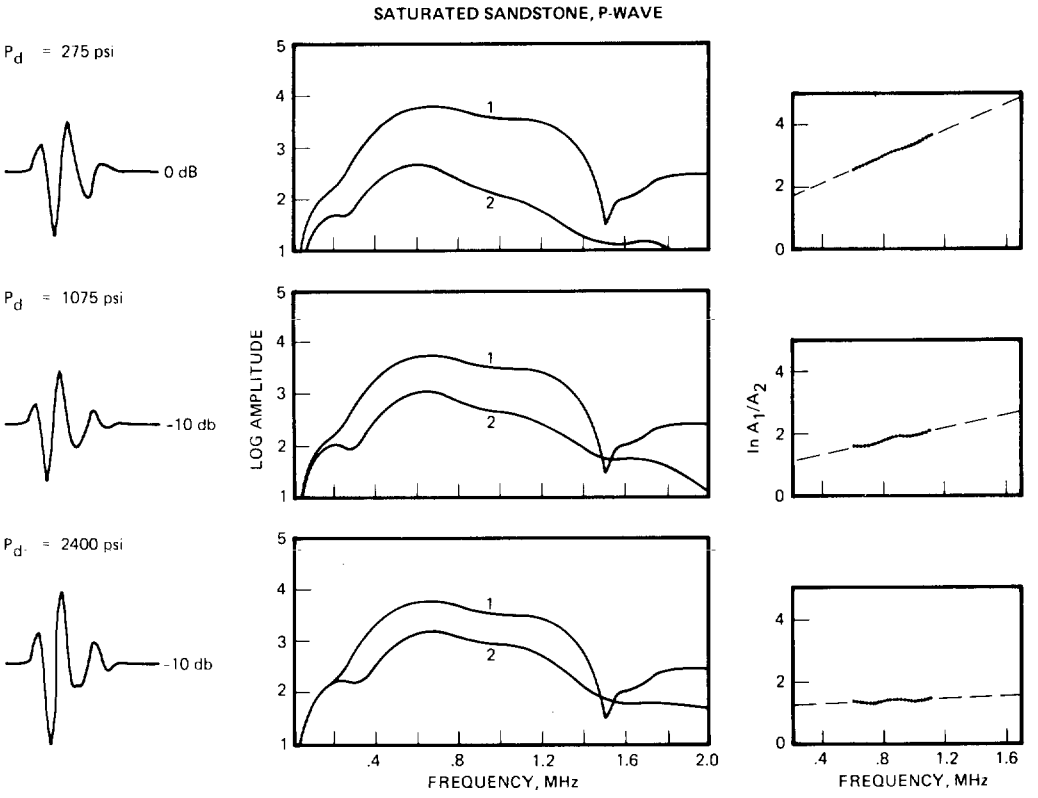

FIG. 8. Attenuation characteristics of P-waves in brine-saturated Berea sandstone for three differential pressures ($P_f = 0.465\ P_c$). Explanations of the different curves are the same as those given in Figure 3.

CONCLUSIONS

We described a laboratory method and presented data on the attenuation of seismic waves in rocks under pressure and in different saturation conditions. The laboratory measurements were made at ultrasonic frequencies (0.1–1.0 MHz). In this frequency range it is shown that:

1) Attenuation coefficients increase linearly with frequency (constant Q) for both P- and S-waves in both dry and saturated rocks. Although our measurement technique of spectral ratios requires that Q be constant, the verification comes from the fact that spectral ratios are linear with frequency over all frequency ranges where the signal-to-noise ratio is high.
2) Attenuation in brine- and water-saturated rocks is greater than in dry or methane-saturated rocks. Attenuation in frozen rocks is very much lower than in saturated rocks.
3) Attenuation decreases (Q increases) with increasing differential pressure both for P- and S-waves in all cases of saturation. The rate of increase is high at low pressures and levels off at higher pressures.
4) In water-saturated rocks, Q_p is higher (10 to 25 percent) than Q_s at both low and high pressures. In dry or methane-saturated rocks, Q_s is slightly higher than Q_p. Since the attenuation coefficient, $\alpha = \pi f/QV$, and the velocity of S-waves is lower than that of P-waves, the attenuation per unit distance of S-waves is higher than that of P-waves in both dry and water-saturated cases.

It is important to mention that the attenuation measurements and conclusions described apply to ultrasonic frequencies of 0.1 – 1.5 MHz and strain amplitudes associated with the pulse technique. Possible variations with frequency and strain amplitude are described in the following paper.

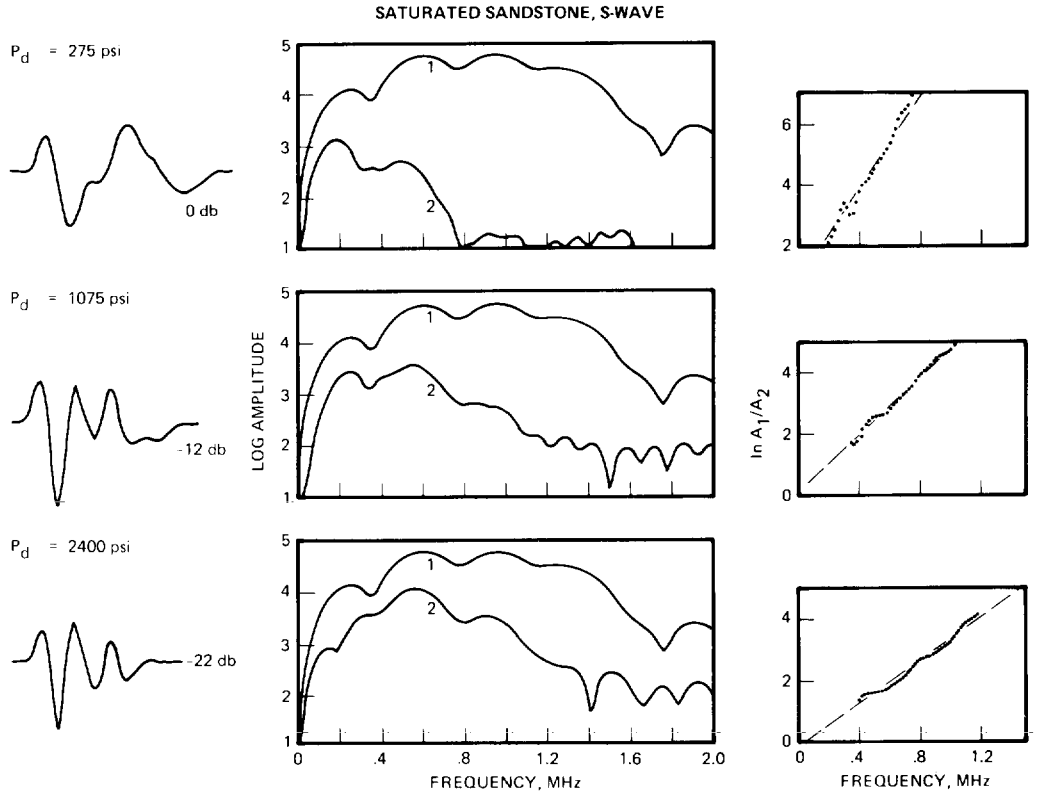

FIG. 9. Attenuation characteristics of *S*-waves in brine-saturated Berea sandstone. Explanations are the same as those in Figure 3.

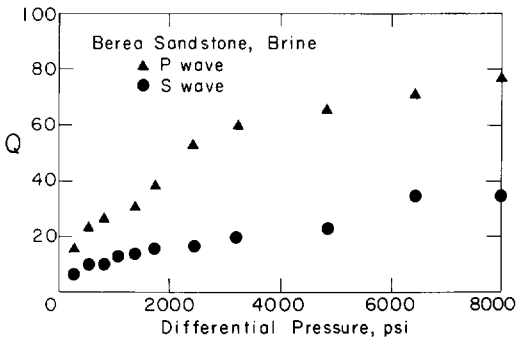

FIG. 10. Q values of P- and S-waves as a function of differential pressure ($P_f = 0.465\,P_c$) in brine-saturated Berea sandstone. The NaCl concentration of the brine is 67,191 ppm.

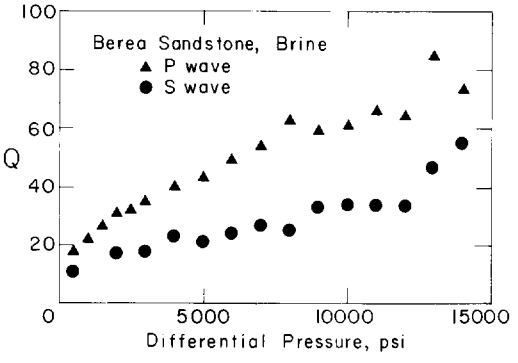

FIG. 11. Q values of P- and S-waves as a function of differential pressure (P_c = 15,000 psi) in brine-saturated Berea sandstone. The NaCl concentration of the brine is 161,334 ppm.

ACKNOWLEDGMENTS

The laboratory measurements described here were done at Chevron Oil Field Research Co., La Habra, California. We thank this company for the release of the data.

REFERENCES

Attewell, P. B., and Ramana, Y. V., 1966, Wave attenuation and internal friction as functions of frequency in rocks: Geophysics, v. 31, p. 1049–1056.

Birch, F., and Bancroft, D., 1938, Elasticity and internal friction in a long column of granite: Bull. SSA, v. 28, p. 243–254.

Born, W. T., 1941, Attenuation constant of earth materials: Geophysics, v. 6, p. 132–148.

Bradley, J. J., and Fort, A. N., Jr., 1966, Internal friction in rocks, *in* Handbook of physical constants: S. P. Clark, Jr., Ed., GSA Publ., p. 175–193.

Gardner, G. H. F., Wyllie, M. R. J., and Droschak, D. M., 1964; Effects of pressure and fluid saturation on the attenuation of elastic waves in sands: J. Petrol. Tech., v. 16, p. 189–198.

Gordon, R. B., and Davis, L. A., 1968, Velocity and attenuation of seismic waves in imperfectly elastic rock: J. Geophys. Res., v. 73, p. 3917–3935.

Hamilton, E. L., 1972, Compressional wave attenuation in marine sediments: Geophysics, v. 37, p. 620–646.

Jackson, D. D., 1969, Grain boundary relaxation and the attenuation of seismic waves: Ph.D. thesis, M.I.T.

Jackson, D. D., and Anderson, D. L., 1970, Physical mechanisms of seismic wave attenuation: Rev. Geophys. Space Phys., v. 8, p. 1–63.

Johnston, D. H., Toksöz, M. N., and Timur, A., 1979, Attenuation of seismic waves in dry and saturated rocks, Part II. Theoretical models and mechanisms: Geophysics, this issue, p. 691–711.

Jones, S. B., Thompson, D. D., and Timur, A., 1977, A unified investigation of elastic wave propagation in crustal rocks: submitted for publication.

Klima, K., Vanek, J., and Pros, Z., 1964, The attenuation of longitudinal waves in diabase and graywacke under pressures up to 4 kilobars: Studia Geoph. et Geod., v. 8, p. 247–254.

Knopoff, L., 1964, Q: Rev. Geophys., v. 2, p. 625–660.

Kuster, G. T., and Toksöz, M. N., 1974, Velocity and attenuation of seismic waves in two-phase media: Part II—Experimental results: Geophysics, v. 39, p. 607–618.

Levykin, A. I., 1965, Longitudinal and transverse wave absorption and velocity in rock specimens at multilateral pressures up to 4000 kg/cm^2: U.S.S.R. Geophys. Ser., Engl. Transl., Phys. Solid Earth, no. 1, p. 94–98.

McDonal, F. J., Angona, F. A., Mills, R. L., Sengbush, R. L., Van Nostrand, R. G., and White, J. E., 1958, Attenuation of shear and compressional waves in Pierre shale: Geophysics, v. 23, p. 421–439.

Nur, A., and Simmons, G., 1969, The effect of viscosity of a fluid phase on velocity in low porosity rocks: Earth Planet. Sci. Lett., v. 7, p. 99–108.

Obert, L., Windes, S. L., and Duvall, W. I., 1946, Standardized tests for determining the physical properties of mine rock: U.S. Bur. Mines R.I. 3891.

Peselnick, L., and Zietz, I., 1959, Internal friction of fine grained limestones at ultrasonic frequencies: Geophysics, v. 24, p. 285–296.

Peselnick, L., and Outerbridge, W. F., 1961, Internal friction and rigidity modulus of Solenhofen limestone over a wide frequency range: USGS Prof. paper no. 400B.

Spetzler, H., and Anderson, D. L., 1968, The effect of temperature and partial melting on velocity and attenuation in a simple binary system: J. Geophys. Res., v. 73, p. 6051–6060.

Timur, A., 1968, Velocity of compressional waves in porous media at permafrost temperatures: Geophysics, v. 33, p. 584–596.

——— 1977, Temperature dependence of compressional and shear wave velocities in rocks: Geophysics, v. 42, p. 950–956.

Tittmann, B. R., Housely, R. M., Alers, G. A., and Cirlin, E. H., 1974, Internal friction in rocks and its relationship to volatiles on the moon: Geochim. et Cosmochim. Acta, Supp. 5, p. 2913–2918.

Toksöz, M. N., Cheng, C. H., and Timur, A., 1976, Velocities of seismic waves in porous rocks: Geophysics, v. 41, p. 621–645.

Tullos, F. N., and Reid, A. C., 1969, Seismic wave attenuation of Gulf Coast sediments: Geophysics, v. 34, p. 516–528.

Warren, N., Trice, R., and Stephens, J., 1974, Ultrasonic attenuation: Q measurements on 70215, 29: Geochim. Cosmochim. Acta. Supp. 5, p. 2927–2938.

Watson, T. H., and Wuenschel, P. C., 1973, An experimental study of attenuation in fluid saturated porous media, compressional waves and interfacial waves: Presented at the 43rd Annual International SEG Meeting, October 22 in Mexico City.

Wyllie, M. R. J., Gardner, G. H. F., and Gregory, A. R., 1962, Studies of elastic wave attenuation in porous media: Geophysics, v. 27, p. 569–589.

Zamanek, J., Jr., and Rudnick, J., 1961, Attenuation and dispersion of elastic waves in a cylindrical bar: J. Acoust. Soc. Am., v. 33, p. 1283–1288.